Materials Today: Proceedings xxx (xxxx) xxx

Contents lists available at ScienceDirect

Materials Today: Proceedings

journal homepage: www.elsevier.com/locate/matpr

Characterization of damage in thermal barrier coating under different thermal cycle

Sachin Sirohi [a], Sanjeev Kumar [a,*], Chandan Pandey [b,*]

[a] SRM Institute of Science and Technology, Modingar 201204, India
[b] Mechanical Department, IIT Jodhpur, Jodhpur 342037, India

ARTICLE INFO

Article history:
Received 6 February 2020
Received in revised form 7 April 2020
Accepted 20 April 2020
Available online xxxx

Keywords:
Thermal barrier coating
Thermal cycle
Ni-Cr
Life prediction
Microstructure

ABSTRACT

Thermal barrier ceramic coatings (TBCs) formed using detonation gun was characterized in this paper. The coating consisted of nickel chromium (Ni-Cr) as bond coat and aluminum oxide (Al_2O_3) as the top coat. The microstructure at interfaces of thermal barrier coating was characterized using the scanning electron microscope (SEM). Thermal cycling have been done for performance evaluation and hot corrosion behaviour of the coatings. Thermally grown oxide layer was developed after few thermal cycles and the thickness of the layer was analysed using SEM. Energy dispersive analysis was used to analyse the elements present in coatings after thermal cycles.

1. Introduction

Thermal barrier coatings (TBCs) are refractory-oxide ceramics coating that bonded with metallic parts to withstand extremely high temperature about 1000 °C [1]. Hence, TBC insulates the material from high temperature and enhance the life of the components. These are two-layer system of coating which consists of insulating outer layer i.e., Top coat and another layer called Bond coat. Bond coat is bounded by the top coat and substrate material which was to be coated. Top coat works as a shielding coat for substrate material to protect it from extreme temperature [2]. The two layers should have minimum difference in thermal expansion coefficient as it leads to stresses and ultimately failure of coating. In general TBC should have high melting, low thermal conductivity, strong tendency to adherence the substrate, chemical inertness, no phase transformation and similar thermal expansion coefficient. The material that are generally used to develop a thermal barrier coating include the NiCoCrAlY, NiCrAlY, NiAl etc. as bond coat material, YSZ, alumina and other advanced ceramics as the top coat material. The operating temperature of the engine in the gas turbine lies in the range of 650–700 °C, and such condition bond coat oxidized and leads to the formation of a new layer, i.e., thermally grown oxide (TGO) layer which is inexorable for extreme temperatures. As the TGO layer grows more, the coating starts sapling that is harmful. Hence, thermal barrier coatings are designed to achieve the slow and uniform growth of TGO layers. Oxygen is less diffusive in this intermediate layer, so it is not a valid reason for controlling the growth of this layer [3]. Failure of TBC may occur in several ways, like the rumpling of the bond coat during exposure to a thermal cycle. Oxidation of thermal barrier coatings leads to reduction of life of substrate drastically due to thermal fatigue. During heating and cooling, thermal barrier coatings expansion & contraction rate are different that results in mismatch in thermal expansion coefficient and it leads to formation of cracks which ultimately leads to failure of coating. The TGO layer growth might be the cause of high residual stresses between top coat and bond coat also leads to deterioration of coatings.

Wang et al. [4] evaluated the thermal expansion coefficient, thermal conductivity, heat insulation, phase composition, and antioxidant ablation of as-sprayed coatings based on $La_{1.7}Dy_{0.3}Zr_2O_7$ (LDZ). It was observed that LDZ could be used effectively as a ceramic layer in the TBC system. Gok et al. [5] designed the Gadolinium Zirconate ($Gd_2Zr_2O_7$) TBC using APS and HVOF processes. The mechanical, microstructural, and thermal properties of the TBC was evaluated. It was investigated that in single layer

* Corresponding authors.
E-mail addresses: sanjeevsrmmech@gmail.com (S. Kumar), jscpandey@iitj.ac.in (C. Pandey).

https://doi.org/10.1016/j.matpr.2020.04.539

$Gd_2Zr_2O_7$large, spallation was observed (74%) after 160 cycles. While in multilayer, the significant improvement observed that no failure was seen even after 300 cycles. Xuet al. [6] presented the factors which affect the interfacial delamination of the TBCs system by using Double Ceramic Layers (DCL). Forces that are responsible for driving crack were examined at the weak interfaces. Song et al. [7] characterized the TBC, fabricated with different layers with lanthanum zirconate (LZO), yttria-stabilized zirconia (YSZ), and YSZ/LZO blended layer and their hot corrosion behavior was predicted in the molten salt environment at 1100 °C. For YSZ/LZO blended layer, different hot corrosion behavior with a relatively shallow depth was observed as compared to LZO and YSZ layers. Thermal cycles have been completed at 755 °C consisting of 100 h duration and followed by 1hr cooling in this way 10 cycles completed in superheater of boilers. Mrowec et al. [8] evaluated the complete oxidation kinetics of metals and alloys. They derived the method for calculating the parabolic rate constant of thermal cycling using the equation by deriving from basic concept of oxidation model.

From literature it is clear that coatings have limited life and they need to be maintained and re-coated properly from time to time for adequate functioning. It also becomes necessary to evaluate the life of the coating. The objective of the present research work is to evaluate the performance of thermal barrier coatings (TBCs) at elevated temperature by thermal cycling. The oxidation behavior of the coatings has been evaluated. The microstructure of thermal barrier coatings at various interfaces using SEM was also assessed. A life prediction model has been developed based on intermediate oxide layer formation to evaluate the life of the TBC.

2. Experimental details

2.1. Thermal barrier coatings material and process

Creep strength martensitic ASTM A335 steel used as a substrate material having composition is listed in Table 1. The samples were prepared by machining the stock P91 material of final thickness 3 mm, round-shaped of diameter 25 mm, as shown in Fig. 1(a). The micrograph of martensitic Cr-Mo steels mainly shows the tempered martensitic microstructure [9]. Al_2O_3 (100%) was used the Top coat powder and Ni-Cr (80%–20%) as the Bond coat powder on the P91 substrate. Specimens are sand blasted for surface roughening so that coating adheres to the substrate correctly. Detonation gun process has been used to coat the sand blasted specimen. Consumption of gases and process parameters are given below in Table 2.

2.2. Thermal cycles phase-I

After thermal barrier coatings, one sample was used in a simple coated condition while the other one was subjected to a molten salt. Sample without coating was also tested. A mixture of Na_2SO_4 and V_2O_5 was taken in the weight ratio 2:3, and distilled water was

Table 2
Specification of D-Gun System.

1	Working Gases	Oxygen, Acetylene, Nitrogen, Air
2	**Pressure of Working Gases**	**MPa**
	Oxygen	0.2
	Acetylene	0.14
	Nitrogen	0.4
	Air	0.4
3	**Consumption of Working gases per shot**	**m^3**
	Oxygen	27×10^{-5}
	Acetylene	23×10^{-5}
	Nitrogen	5×10^{-4}
	Air	5×10^{-4}
4	Consumption of powder per shot	0.05–0.02 g/shot
5	Water Consumption Rate	15–20 L/ minute
6	Firing Rate	1–10 Hz
7	Dia. of accelerating portion of barrel or coating coverage	0.022 *m*
8	Coating thickness per shot	5–25 μm
9	Coating capacity at the rate of 7 μm/shot	0.75 m^2/h
10	**System Control**	**Manual / Automatic**
	Gun dimension	1.8×1.1
	Control Console dimension	$1.2 \times 0.5 \times 1.5$
11	**Power supply from mains**	
	Frequency	50–60 Hz
	Voltage	430 V
	Power	450 VA
12	Sound Pressure level	150 dB
13	Relative humidity of ambient air	50%

Table 1
Chemical composition of P91 Steel, wt.%.

Element	Cr	C	Mn	Mo	N	V	N	Si	Ni	Cu	Fe
wt.%	8.48	0.11	0.54	0.95	0.06	0.18	0.02	0.28	0.35	0.06	Re

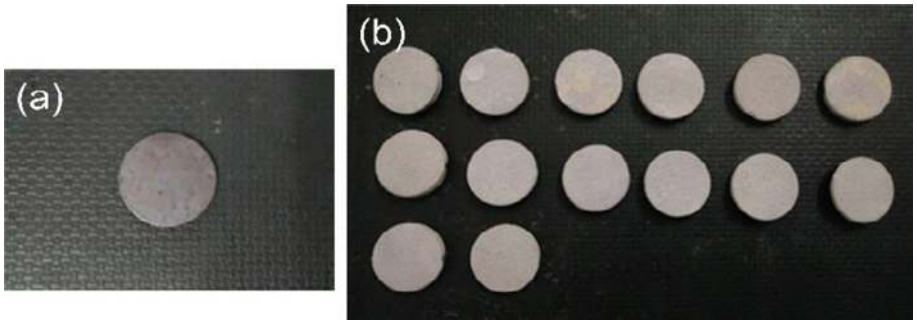

Fig. 1. (a) Initial coated sample, (b) coated Samples.

Please cite this article as: S. Sirohi, S. Kumar and C. Pandey, Characterization of damage in thermal barrier coating under different thermal cycle, Materials Today: Proceedings, https://doi.org/10.1016/j.matpr.2020.04.539

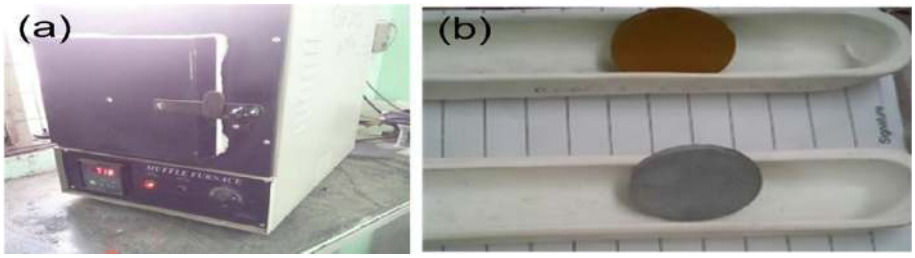

Fig. 2. (a) Muffle furnace, (b) crucible like alumina boats.

Fig. 3. Samples after thermal cycle for fracture toughness.

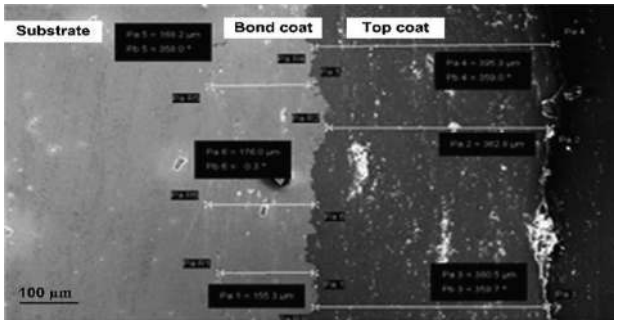

Fig. 4. SEM image showing coating thickness.

used to diffuse the salt so that a 50 wt% salt solution could be obtained. The sample was subjected to a molten salt solution as per reference [10].

Initially, the weight of the coated specimen was measured and preheated at 200 °C for 30 min to get great bonding of salt onto the coated sample. After preheating, solution was applied by a camel thin hair brush. The salt coated specimen put in the muffle furnace at 100 °C for 1 h to evaporate the moisture contents. The muffle furnace is shown in Fig. 2(a). The salt coated specimen weighted to measure the quantity of salt accumulated/unit area to get a concentration of 3–5 mg/cm^2. Two more specimens are used one was simply coated and other was without coating. Before initiating the hot corrosion test each specimen were placed in crucible like alumina boats as shown in Fig. 2(b), and combined weight of boat and specimen was measured. Samples were placed in a muffle furnace at 700 °C for 80 min, cooling time for 1 cycle. In the step of 20 min of cycle, 50 cycles was conducted and weight gain was measured after every cycle.

2.3. Thermal cycles phase-II

In this phase, first two samples prepared for thermal cycling: one was stock coated and other one was subjected to molten salt and samples were placed in alumina boats. Salt preparation method was same as in previous step. In this thermal cycle consists of 10 min heating at 700 °C followed by 10 min force cooling. In phase II, thermal cycle remain continue till 20% of coating failure. After the failure of 20% coating area, thermal cycles stopped and thermally grown oxide layer thickness was measured. In next step, three samples were taken and applied molten salt and subjected to thermal cycles first at 20 cycle, second at 40 cycle, third at 60 cycles and then stopped. Similarly, 3 more samples taken without application of molten salt and subjected to first one at 30 cycle, second at 60 cycle, third at 90 cycles and stopped. Now these 6 samples (3 salt + coat and 3 w/o salt + coat) analysed for TGO growth as shown in Fig. 3.

2.4. Characterization

Field Emission Scanning Electron Microscope (FE-SEM) was used to examine the samples after thermal cycling for evaluating the microstructure, morphology of the surface, and thickness of coatings on the cross section of samples. After the thermal cycle's completion, both the samples were cut using slow-speed diamond cutter and subjected to cross-section analysis using the SEM, and EDAX after proper mirror polishing using different grades of emery papers.

3. Results and discussion

3.1. Characterization of coated samples

The SEM image of coated sample is shown in Fig. 4. The top and bond coat thickness were measured 360–400 μm and 150–200 μm, respectively. SEM image was used to analyse the stock coating. The EDS spectrums were taken at different location and shown in Fig. 5. The spectrum in top coat (Fig. 5b) only consists of aluminium and oxygen than confirms the presence of aluminium oxide (Al_2O_3) in top coat. The EDS spectra in bond coat confirms the presence of primarily carbon, nickel, chromium, and oxygen element, as shown in Fig. 5(c). The interface layer (TGO layer) shows the evolution of aluminum oxide from top coat and also nickel, chromium from the bond coat, as shown in Fig. 5(d).

3.2. Characterization of samples after 50 thermal cycles

After the thermal cycles sample were characterized using the FESEM. The (TGO) layer was formed between Al_2O_3 coat and, Ni-Cr coat and the thickness of this layer was measured about 8.21 μm as shown in Fig. 6. The EDS spectrum was taken in TGO layer and elements and presented in Table 2. After completion of

Please cite this article as: S. Sirohi, S. Kumar and C. Pandey, Characterization of damage in thermal barrier coating under different thermal cycle, Materials Today: Proceedings, https://doi.org/10.1016/j.matpr.2020.04.539

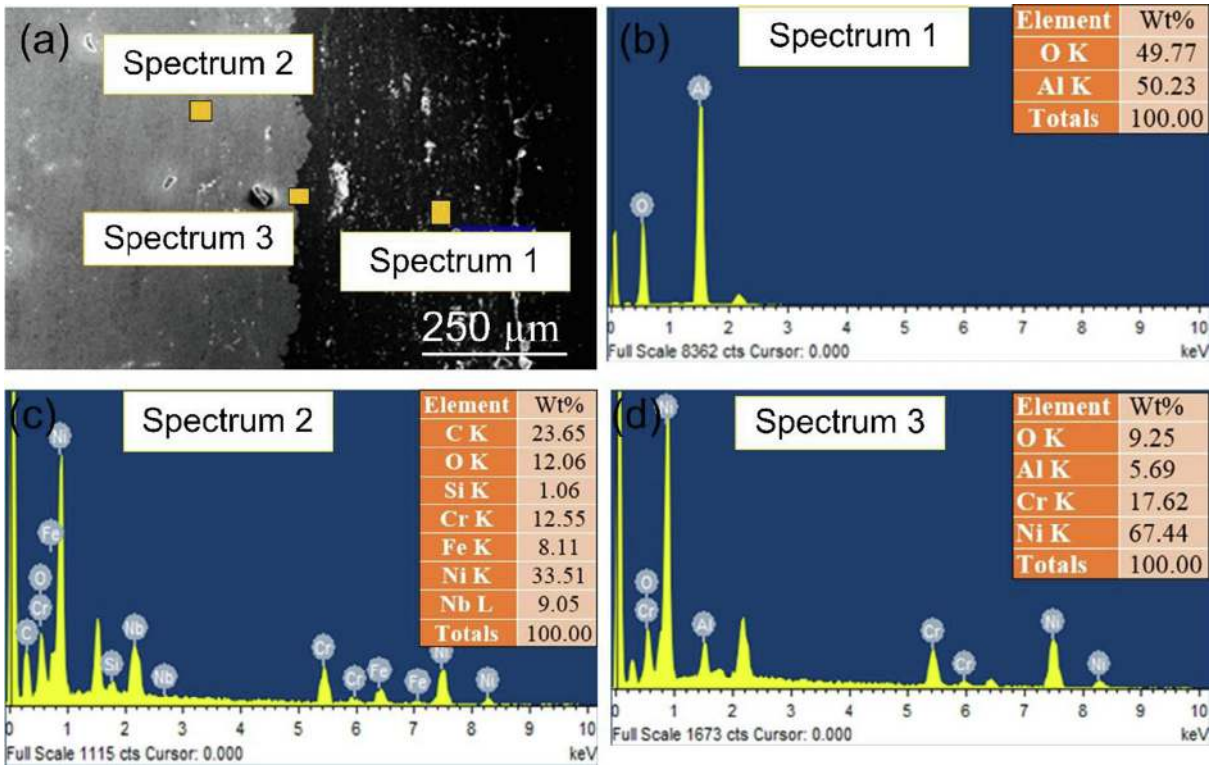

Fig. 5. (a) SEM image showing location of EDS spectra, (b) EDS spectra at top coat, (c) EDS spectra at bond coat, (d) EDS spectra at interface.

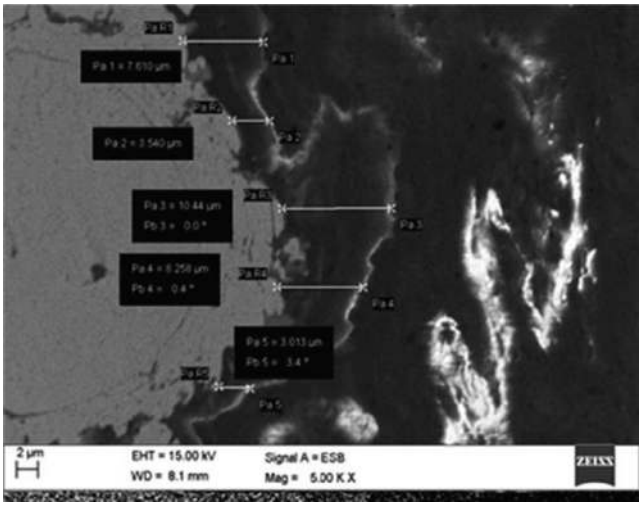

Fig. 6. TGO layer thickness.

50 thermal cycles, the cross section was analysed by SEM for coating analysis and presented in Fig. 7. Fig. 7(a) shows the crack in Al_2O_3 coating i.e., Top coat near the interface between two coatings. The crack in Al_2O_3 coating occurs mainly due to oxide layer formation. Fig. 7(b) shows that the sample exposed to molten salt after 50 TC have left with a very small layer of Top coat and thickness was measured about 10 μm. This might be due to the spinal in coating, and also molten salt accelerated the oxidation rate, which further led to the spalling of the coating.

The area elemental mapping for coated sample without salt, after thermal cycle is shown in Fig. 8. The higher concentration of Al and O in bond coat and top coat were observed. That confirms the oxide layer formation in top and bond coat. In bond coat, mainly concentration of Ni and Cr particles are observed.

In salt bath condition, higher concentration of Al and O in top coat confirms the formation of Al_2O_3. In bond coat Ni-Cr layer formation is observed. In salt bath condition, higher concentration of Al and O in top coat confirms the formation of Al_2O_3. It confirms the TGO formation between Al_2O_3 coat and Ni-Cr coat.

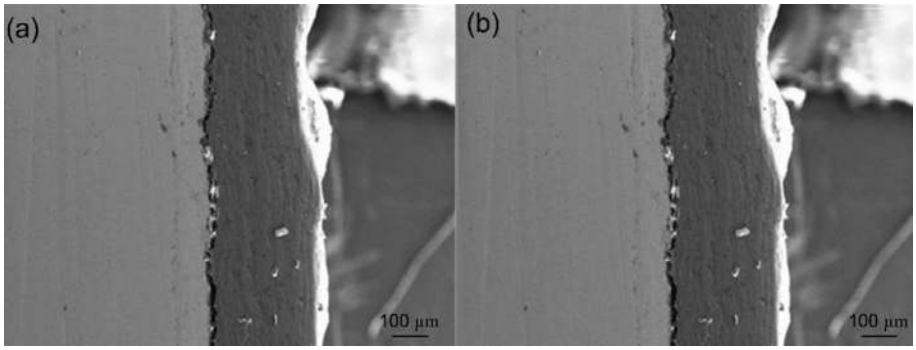

Fig. 7. (a) Coated Sample w/o salt after 50 TC, (b) with salt after 50 TC.

Please cite this article as: S. Sirohi, S. Kumar and C. Pandey, Characterization of damage in thermal barrier coating under different thermal cycle, Materials Today: Proceedings, https://doi.org/10.1016/j.matpr.2020.04.539

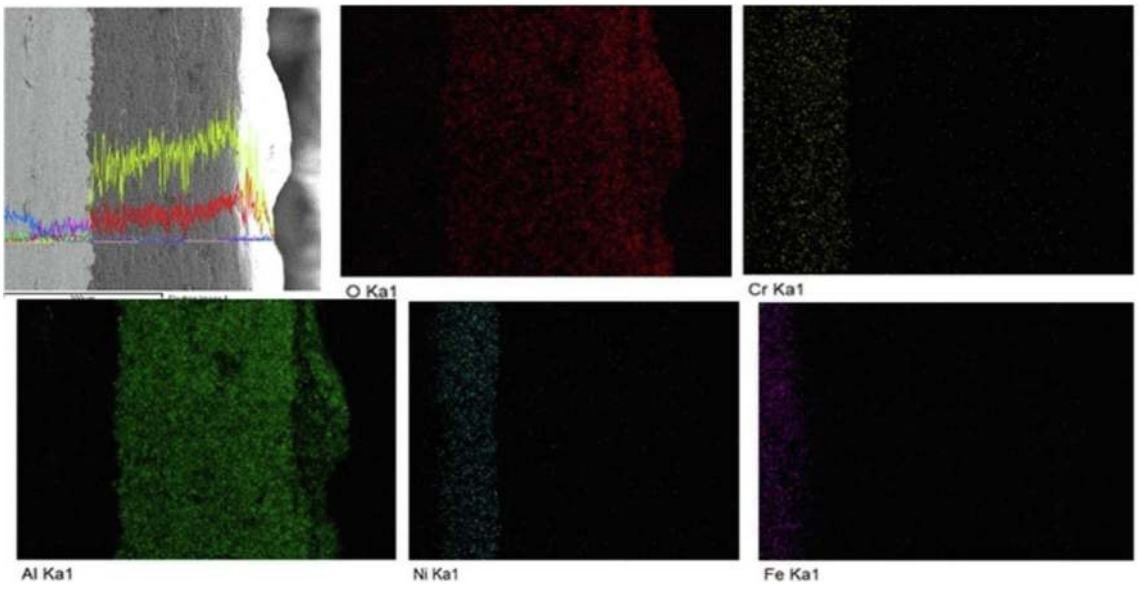

Fig. 8. Line and area elemental mapping for coated sample w/o salt after 50 TC.

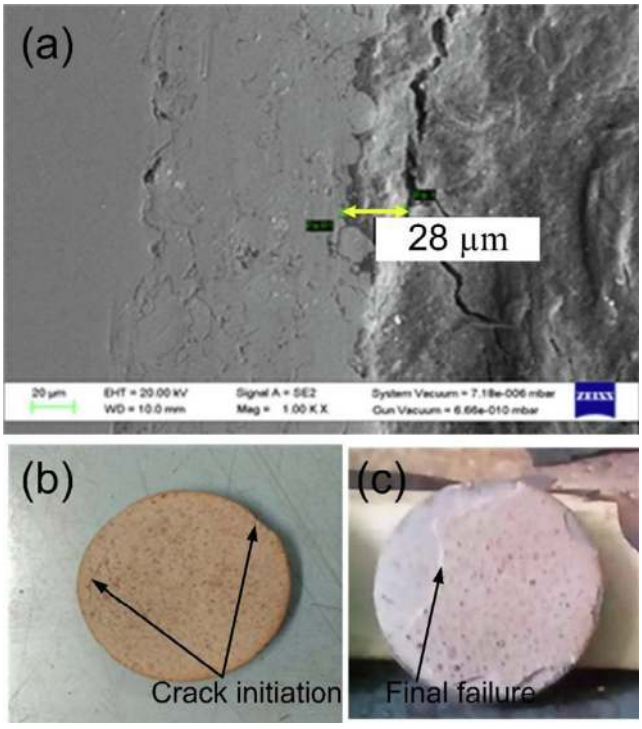

Fig. 9. (a) Sample after 298 cycles shows crack, (b) first crack appeared after 200 cycles, (c) coating failed after 298 cycles.

3.3. Characterization of the samples subjected to thermal cycles up to fracture

Fig. 9(a) shows the crack developed near the interface (approximately 28 μm) above in top coat region which was responsible for failure of the coating. The failure occurs due to formation of spinels and penetration of oxides near the interface through micro cracks and porosity. A white oxide layer also formed at the interface that indicates the other region of spalling of coating. Initially crack developed after the 298 cycles (Fig. 9(b)) and propagate and final fracture occur after the 298 cycles (Fig. 9(c)). The area mapping (Fig. 10) confirms the higher concentration of Al and O in top coat layer and it also confirms the formation of the oxide layer. However, the interface was noticed to be rich in Ni. Along the bond coat, higher concentration of Cr and Fe particles was measured. SEM image of the coated sample exposed in molten salt bath is shown in Fig. 11(a). Molten salt accelerated the oxidation rate of coating and resulted in crack propagation and crack appeared above the interface in top coat only after 97 cycles. The crack initiation occurs mainly due to the rapid oxidation and TGO formation at the interface. The sample with crack appearance after the 66 thermal cycles is shown in Fig. 11(b).

4. Conclusions

Performances of thermal barrier coatings have been evaluated by analyzing the oxidation behavior of these coatings at 700 °C. The following findings are summarized:

- The top and bond coat thickness was measured 360–400 μm and 150–200 μm, respectively.
- The interface layer (TGO layer) showed the evolution of aluminum oxide from top coat and nickel, chromium from the bond coat and thickness was measured about 8.21 μm
- Crack in Al_2O_3 coating was noticed after 50 thermal cycle, and it occurs mainly due to oxide layer formation.
- The samples subjected to the thermal cycle up to final fracture shows the crack of length approximately 28 μm and considered as the responsible factor for the failure of the coating. The initial fracture was noticed after the 200 cycles while final fracture of the coating was observed after the 298 cycles.
- In molten salt condition, a crack was appeared above the interface in top coat only after 97 cycles, and it was attributed to rapid oxidation and TGO formation at the interface.

Please cite this article as: S. Sirohi, S. Kumar and C. Pandey, Characterization of damage in thermal barrier coating under different thermal cycle, Materials Today: Proceedings, https://doi.org/10.1016/j.matpr.2020.04.539

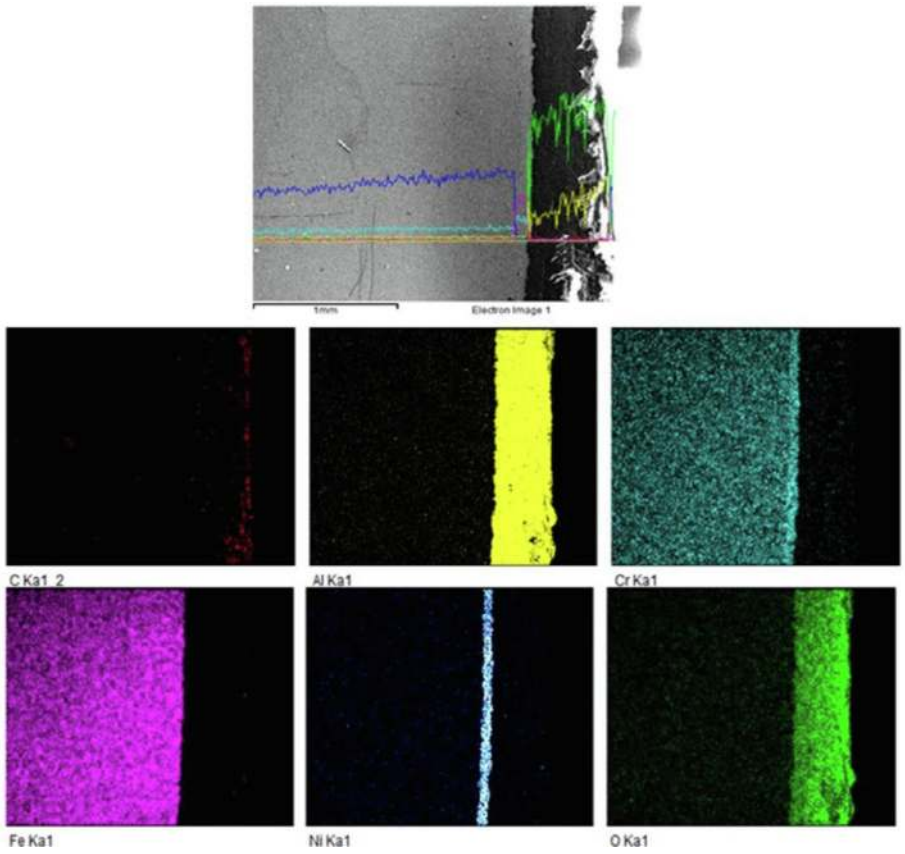

Fig. 10. Area elemental mapping for coated sample without salt.

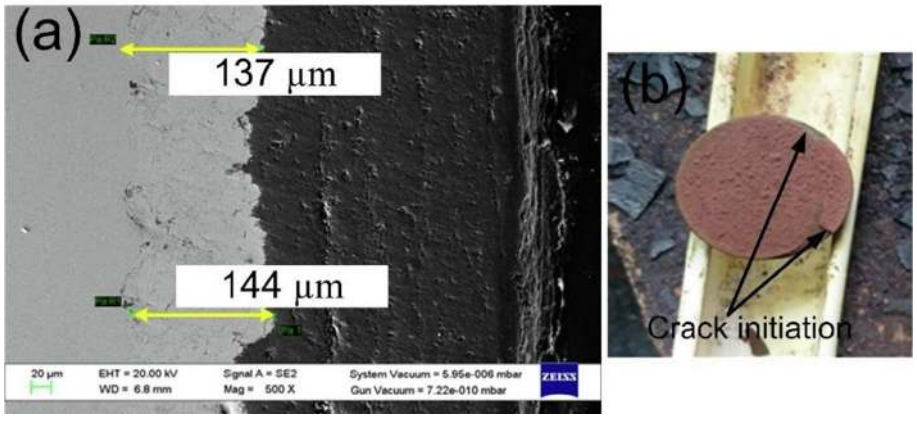

Fig. 11. (a) SEM image of the sample with molten salt after 97 cycles, (b) crack appeared after 66 thermal cycles.

Declaration of interests

No conflict of interest.

CRediT authorship contribution statement

Sachin Sirohi: Conceptualization, Methodology. **Sanjeev Kumar:** Supervision. **Chandan Pandey:** Visualization, Investigation.

References

[1] G. Mehboob, M.J. Liu, T. Xu, S. Hussain, G. Mehboob, A. Tahir, A review on failure mechanism of thermal barrier coatings and strategies to extend their lifetime, Ceram. Int. (2009).
[2] D.R. Clarke, S.R. Phillpot, Thermal barrier coating materials, Mater. Today, Elsevier Ltd 8 (6) (2005) 22–29.
[3] N.P. Padture, M. Gell, E.H. Jordan, Thermal barrier coatings for gas-turbine engine applications, Science 80 296 (2002) 280–284.
[4] X. Wang, S. Guo, L. Zhao, Y. Zhu, L. Ai, A Novel thermal barrier coating for high-temperature applications, Ceram. Int. 42 (2) (2016) 2648–2653.

Please cite this article as: S. Sirohi, S. Kumar and C. Pandey, Characterization of damage in thermal barrier coating under different thermal cycle, Materials Today: Proceedings, https://doi.org/10.1016/j.matpr.2020.04.539

[5] M. Guven Gok, G. Goller, Production and characterisation of GZ/CYSZ alternative thermal barrier coatings with multilayered and functionally graded designs, J. Eur. Ceram. Soc., Elsevier Ltd 36 (7) (2015) 1755–1764.
[6] R. Xu, X. Fan, T.J. Wang, Mechanisms governing the interfacial delamination of thermal barrier coating system with double ceramic layers, Appl. Surf. Sci., Elsevier B.V. 370 (2016) 394–402.
[7] D. Song, T. Song, U. Paik, G. Lyu, Y.G. Jung, Hot corrosion behavior in thermal barrier coatings with heterogeneous splat boundary, Corros. Sci. 163 (2016).
[8] S. Mrowec, A. Stokłosa, Calculations of parabolic rate constants for metal oxidation, Oxid. Met. 8 (6) (1974) 379–391.
[9] C. Pandey, Mechanical and metallurgical characterization of dissimilar P92/SS304 L welded joints under varying heat treatment regimes, Metall. Mat. Trans. A 51 (2020) 2126–2142.
[10] W.R. Chen, R. Archer, X. Huang, B.R. Marple, TGO growth and crack propagation in a thermal barrier coating, J. Therm. Spray Technol. 17 (5–6) (2008) 858–864.

Please cite this article as: S. Sirohi, S. Kumar and C. Pandey, Characterization of damage in thermal barrier coating under different thermal cycle, Materials Today: Proceedings, https://doi.org/10.1016/j.matpr.2020.04.539